6-29-2016

Computational Code for Optimization of Thermal Treatment of Fine Grained Soils as a Method of Expediting their Load Induced Consolidation

Radhavi Abeysiridara Samarakoon
University of South Florida, radzsam@gmail.com

Computational Code for Optimization of Thermal Treatment of Fine Grained Soils as a Method of Expediting their Load Induced Consolidation

by

Radhavi Abeysiridara Samarakoon

A thesis submitted in partial fulfillment
of the requirements for the degree of
Master of Science in Civil Engineering
Department of Civil and Environmental Engineering
College of Engineering
University of South Florida

Major Professor: Manjriker Gunaratne, Ph.D.
Gray Mullins, Ph.D.
Andres Tejada-Martinez, Ph.D.

Date of Approval:
June 24, 2016

Keywords: Vertical Drains, Settlement, Thermal Yielding, Soft Ground Improvement, Thermoplasticity

TABLE OF CONTENTS

LIST OF TABLES

LIST OF FIGURES

ABSTRACT

Construction in soft soils has been a challenging task for engineers due to the excessive time taken for dissipation of construction induced pore water pressure and the ensuing post-construction settlement. Use of vertical drains has proven to be an effective and economical method for soft ground improvement and hence extensive research has been carried out to further improve its efficiency. Effect of temperature on radial consolidation is one aspect of such research among many others that have been pursued.

Elevated temperature certainly has a pronounced effect on the hydraulic conductivity due to the reduction it causes in the viscosity of water. Furthermore, temperature also generates excess pore water pressure due to the tendency for differential volumetric expansion between the soil grains and pore water. Thermally induced volumetric strains can have an effect on the magnitude of settlement as well. A numerical methodology based on the Navier-Stokes equations of flow and thermoelasto-plastic soil compressibility relationships was developed to model transient fluid flow in a clay under thermal treatment. Experimentally verified soil compressibility relationships coupling the loading and thermal effects obtained from literature were employed in this model. The transient temperature distribution within the consolidation soil was modeled using the Fourier's equation of heat transfer.

The effect of temperature on consolidation of clay was investigated by a parametric study involving different maximum temperatures, surcharge loads and initial porosities of clay.

It was concluded that the improvement in the magnitude and rate of settlement at elevated temperature is more significant at relatively smaller surcharges and low initial porosities. Since there is a possibility for thermally induced volumetric expansion even in normally consolidated clays, an optimum combination of surcharge and thermal treatment should be employed for given initial conditions of the soil, in order to achieve the maximum improvement in settlement. The developed numerical model will provide the framework to carry out further investigations and determine the viability of the practical implementation of coupled thermomechanical consolidation using prefabricated vertical drains.

CHAPTER 1: INTRODUCTION

Consolidation settlement is an important design consideration when constructing foundations on soft soil. When a saturated partially draining soil layer is subjected to an increase in overburden stress, excess pore water pressure is generated. This creates a hydraulic gradient between that layer and other well drained soil layers and the excess pore water pressure is dissipated over time until the applied stress is transferred to the soil grains. The volumetric compression that occurs due to the expulsion of pore water is referred to as consolidation. Although this process takes place rapidly in coarse-grained soils with high permeability, it occurs over a long period in low permeable soils such as clay. Therefore, settlements due to consolidation can be problematic when constructing on clayey soils.

Pre-consolidation by pre-loading is used as a means of overcoming long-term settlement problems encountered when constructing on clayey soils. In usual practice, a surcharge exceeding the expected construction load is added to the soil prior to construction and allowed to settle in order to avoid undesirable post-construction settlements. More recently, use of prefabricated vertical drains (PVDs) has been widely proven as an effective and economical method for pre-consolidation and soft ground improvement. Vertical drains accelerate the consolidation process by shortening the drainage path through the soil and allowing the water to flow out vertically through the drain. In addition, it utilizes the relatively higher horizontal permeability of clay.

Thermomechanics of clay associated with nuclear waste deposits in clayey barrier material has been investigated extensively for decades by many researchers. However, the application of thermomechanics of soils for ground improvement was first proposed by Abuel-Naga, Bergado, & Chaiprakaikeow (2006) where a heat source was combined with a PVD. This innovative thermal technique can be used to achieve faster rates of consolidation as well as higher magnitudes of settlements due to the increased permeability and collapsing of clay structure under an increased temperature respectively. Many laboratory and field scale experiments have been carried out to verify and validate the effect of temperature on soil properties, consolidation rate and the magnitude of settlement (Abuel-Naga, Bergado, & Chaiprakaikeow, 2006; Pothiraksanon, Bergado, & Abuel-Naga, 2010; Artidteang, Bergado, Saowapakpiboon, Teerachaikulpanich, & Kumar, 2011).

The objective of this research is to develop a computational tool to optimize the thermal treatment of soft soils to expedite the consolidation process.

1.1 Background

Methods of expediting consolidation of soft soils have been studied by many engineers. Pre-consolidation using vacuum and thermal PVDs where a surcharge is applied in combination with vacuum pressure and a heat source respectively, are two such widely investigated techniques. Experimental studies conducted by Artidteang, Bergado, Saowapakpiboon, Teerachaikulpanich, & Kumar (2011) and Saowapakpiboon, Bergado, Thann, & Voottipruex (2009) where the impact on consolidation settlement with a vacuum-PVD and thermo-PVD was compared showed that the use of a thermo-PVD not only increased the rate of settlement but

also the magnitude of settlement. Therefore, it can be seen that the effect of temperature on consolidation settlement is twofold.

1. Enhancing the rate of settlement, and
2. Increasing the magnitude of settlement

1.2 Effect of Temperature on Rate of Settlement

Based on the discussion in section 1.1, the rate of settlement will be determined by the rate of pore water pressure dissipation. The rate at which pore water pressure dissipates depends on the instantaneous hydraulic gradient created and the hydraulic conductivity of the soil. With an increase in temperature of the soil medium, two main phenomena can be observed.

1. Increase in hydraulic conductivity due to a decrease in viscosity of water
2. Generation of excess pore water pressure due to differential expansion between the soil grains and pore water, which increases the hydraulic gradient

Therefore, it is evident how a temperature increase would have a significant effect on the rate of settlement.

1.2.1 Effect of Temperature on Hydraulic Conductivity

Hydraulic conductivity refers to the ease with which water can flow through porous media and can be expressed as in equation 1.

$$k = \frac{K\gamma}{\mu} \quad (1)$$

where k is the hydraulic conductivity, K is the intrinsic hydraulic conductivity (or permeability), γ is the unit weight of water and μ is the viscosity of water. Research by Abuel-Naga, Bergado, & Chaiprakaikeow (2006) indicates an increase in hydraulic conductivity with an increase in temperature attributed to the corresponding decrease in viscosity of water. The relationship between temperature and water viscosity has been given by Hillel (1980) and Abuel-Naga, Bergado, & Chaiprakaikeow (2006) as indicated in equation 2 with water viscosity in Pa.s and temperature in °C.

$$\mu(T) = -0.00046575 \ln(T) + 0.00239138 \quad (2)$$

1.2.2 Effect of Temperature on Pore Water Pressure

The excess pore water pressure generated under an applied surcharge will create a hydraulic gradient which in turn will initiate water flow through the soil. In an entirely surcharge driven consolidation process, excess pore water pressure is generated by an increase in overburden stress. However, when coupled with a heat source, an increase in temperature can also generate excess pore water pressure. Soil is a composite material consisting of soil grains and water. There is a significant difference between the thermal expansion coefficients of water and soil grains with that of water being much higher. As a result, when a soil mass is heated under undrained conditions, excess pore water pressure would be generated due to the tendency for differential volumetric expansion.

This phenomena can be illustrated analytically by considering a dry soil skeleton subject to a temperature increase of ΔT, the final volume of voids, V_v can be expressed by equation 3.

$$V_v = V_0(1 + \beta_{soil})\Delta T \quad (3)$$

where V_0 is the initial volume of voids and β_{soil} is the thermal expansion coefficient of the soil grains. If the pores are saturated with water, the volume of water after a temperature increment of ΔT would be given by equation 4.

$$V_w = V_0(1 + \beta_{water})\Delta T \quad (4)$$

where V_w is the final volume of voids and β_{water} is the thermal expansion coefficient of water.

Therefore, the differential volumetric expansion tendency can be expressed by equation 5.

$$\Delta V = V_w - V_v = V_0(\beta_{water} - \beta_{soil})\Delta T \quad (5)$$

The expansion coefficient of soil grains can be considered negligible compared to that of water. Hence, the differential volumetric expansion tendency can be expressed as the expansion of pore water for the corresponding temperature increment.

1.3 Effect of Temperature on the Magnitude of Settlement

Extensive experimental research has been conducted on the thermomechanical behavior of clays and all studies conclusively indicate that the thermally induced volumetric change of saturated fine grained soils is stress history dependent where normally consolidated (NC) clays contract irreversibly and highly over consolidated (OC) clays expand reversibly (Robinet, Rahbaoui, Plas, & Lebon, 1996; Abuel-Naga, Bergado, Bouazza, & Ramana, 2007). A shift in the virgin compression line to the left with similar slope was observed during isothermal consolidation at different elevated temperatures. It was also observed that an over consolidated state is induced in NC clays after being subject to a heating cooling cycle.

Thermomechanical models reflecting the experimentally observed behavior of saturated clays at elevated temperatures have been developed by several researchers (Robinet, Rahbaoui, Plas, & Lebon, 1996; Cui, Sultan, & Delage, 2000; Laloui & Cekerevac, 2003; Abuel-Naga, Bergado, Bouazza, & Ramana, 2007) and the irreversible contractive volume change behavior was attributed to thermal yielding of the soil at elevated temperatures. This research incorporates the model proposed by Abuel-Naga, Bergado, Bouazza, & Ramana (2007). The model delineates thermoelasto-plastic and thermo-elastic regions based on the contractive and dilative behavior of the soil as it changes from NC to OC states respectively. The stress at the stage separating the thermo-elastic and thermoelasto-plastic regions is referred to as the thermal yield limit at the respective elevated temperature. Therefore, an increase in temperature can affect the magnitude of the settlement due to the volume change behavior resulting from the thermal yielding of soil.

CHAPTER 2: NUMERICAL MODEL

The consolidation process with thermal effects was first modeled in order to investigate the effect on settlement of fine grained soils. With prefabricated vertical drains (PVD) being used for pre-consolidation, it was assumed that the heat source will be installed at the location of the drain and throughout its depth. Therefore, with radial flow and temperature distribution around a drain, the model can be considered to be axisymmetric about the axis of the drain. Furthermore, assuming no variation in temperature in the vertical direction, it can be simplified to a one dimensional radial flow problem. When modeling the consolidation process, transient fluid flow through porous media and the compressibility characteristics of the soil skeleton appropriately modified for thermal effects were considered.

2.1 Modeling the Fluid Flow

The transient fluid flow was modeled using the two Navier-Stokes (NS) equations, modified to account for temperature changes. The NS equations can be derived for a finite element along a radius considering a variation in density due to a change in temperature.

2.1.1 Continuity Equation

Considering radial flow through a finite element, equation 6 can be written for the mass balance of the element.

$$(\rho nu)rd\theta dz - \left[\rho nu + \frac{\partial(\rho nu)}{\partial r}dr\right](r + dr)d\theta dz = \frac{\partial(\rho nrd\theta drdz)}{\partial t} \quad (6)$$

where r is the radial distance to the element, u is the water velocity in the radial direction, n is the porosity of the soil and ρ is the density of water. Equation 6 can be simplified to equation 9 as follows.

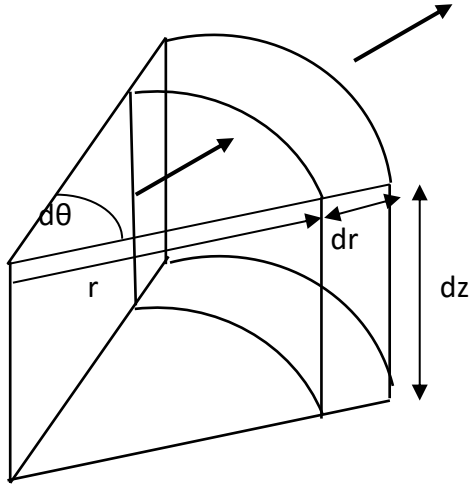

Figure 2.1 Flow through a finite radial element

$$-\rho nudrd\theta dz - \frac{\partial(\rho nu)}{\partial r}dr\, rd\theta dz = rd\theta drdz\frac{\partial(\rho n)}{\partial t} \quad (7)$$

$$-\rho nu - r\frac{\partial(\rho nu)}{\partial r} = r\frac{\partial(\rho n)}{\partial t} \quad (8)$$

$$-\frac{\rho nu}{r} - \rho\frac{\partial(nu)}{\partial r} - nu\frac{\partial(\rho)}{\partial r} = \rho\frac{\partial n}{\partial t} + n\frac{\partial \rho}{\partial t} \quad (9)$$

The Boussinesq approximation (Cengel & Cimbala, 2006) can be used in place of the fully compressible Navier-Stokes equations, to account for small density variations in non-isothermal flow. The density variation can be considered as given in equation 10 with reference density ρ_0.

$$\rho = \rho_0 + \rho' \text{ with } \rho' \ll \rho_0 \quad (10)$$

ρ' is the variation in density due to a ΔT change in temperature and can be expressed as in equation 11.

$$\rho' = -\rho_0 \beta \Delta T \tag{11}$$

where β is the thermal expansion coefficient of water.

By substituting equation 10 into equation 9, the following equation can be obtained.

$$-\frac{(\rho_0+\rho')nu}{r} - (\rho_0 + \rho')\frac{\partial(nu)}{\partial r} - nu\frac{\partial(\rho_0+\rho')}{\partial r} = (\rho_0 + \rho')\frac{\partial n}{\partial t} + n\frac{\partial(\rho_0+\rho')}{\partial t} \tag{12}$$

Since $\rho' \ll \rho_0$ and ρ_0 is constant, it can be further simplified as follows.

$$-\frac{\rho_0 nu}{r} - \rho_0\frac{\partial(nu)}{\partial r} - nu\frac{\partial\rho'}{\partial r} = \rho_0\frac{\partial n}{\partial t} + n\frac{\partial\rho'}{\partial t} \tag{13}$$

Generally, with Bousinessq approximation, the magnitude of the material derivative is considered negligible compared to the velocity gradients. However, in this instance where seepage through porous media is considered, only the spatial term of the material derivative is disregarded. Substituting equation 11 and neglecting small terms, the final form of the continuity equation is as in equation 14.

$$-\frac{nu}{r} - \frac{\partial(nu)}{\partial r} = \frac{\partial n}{\partial t} + n\beta\frac{\partial T}{\partial t} \tag{14}$$

2.1.2 Momentum Equation

Similarly, the momentum equation can be obtained for a finite radial element considering the balance of momentum. Neglecting convective acceleration, it will be as in equation 15 for radial flow (Jeyisanker & Gunaratne, 2008; Bird, Stewart, & Lightfoot, 1960).

$$\mu\frac{\partial\left[\frac{1}{r}\frac{\partial(rnu)}{\partial r}\right]}{\partial r} - n\frac{\partial p}{\partial r} + D_r = \frac{\partial(\rho nu)}{\partial t} \tag{15}$$

where μ is the viscosity of water, p is the pressure and D_r is the drag force per unit volume of water which is obtained from equation 16.

$$D_r = -c\mu\left(\frac{1-n}{n}\right)^2\left(\frac{1}{{d_p}^2}\right)u \tag{16}$$

where $d_p$is the average particle size and c is a particle shape dependent constant which is 150 for spherical particles.

Using the Boussinesq approximation (Cengel & Cimbala, 2006), equation 15 will simplify as follows.

$$\mu\frac{\partial\left[\frac{1\partial(rnu)}{r\ \partial r}\right]}{\partial r} - n\frac{\partial p}{\partial r} + D_r = \rho\frac{\partial(nu)}{\partial t} + nu\frac{\partial(\rho)}{\partial t} \tag{17}$$

$$\mu\frac{\partial\left[\frac{1\partial(rnu)}{r\ \partial r}\right]}{\partial r} - n\frac{\partial p}{\partial r} + D_r = (\rho_0 + \rho')\frac{\partial(nu)}{\partial t} + nu\frac{\partial(\rho_0+\rho')}{\partial t} \tag{18}$$

Since $\rho' \ll \rho_0$, the $\rho'\frac{\partial(nu)}{\partial t}$ term can be neglected. The $nu\frac{\partial\rho'}{\partial t}$ term can be simplified to give $nu\rho_0\beta\frac{\partial T}{\partial t}$ using equation 11, and as the velocity term multiplied by the thermal expansion coefficient of water will generate a small value given the slow flows expected, this term too can be neglected. The final form of the momentum equation is given below where equation 16 has been substituted for D_r.

$$\frac{\mu}{\rho_0}\frac{\partial\left[\frac{1\partial(rnu)}{r\ \partial r}\right]}{\partial r} - \frac{n}{\rho_0}\frac{\partial p}{\partial r} - 150\mu\left(\frac{1-n}{n}\right)^2\left(\frac{1}{{d_p}^2}\right)u = \frac{\partial(nu)}{\partial t} \tag{19}$$

2.2 Modeling the Compressibility Characteristics of Soil

The thermomechanical model proposed by Abuel-Naga, Bergado, Bouazza, & Ramana (2007) was used in this research to model the compressibility behavior of the soil subject to thermal loading. In the above work, they have introduced a thermal yield limit in addition to

the loading yield limit (pre-consolidation pressure). The evolution of the thermal yield limit with temperature is expressed by the following relationship.

$$\frac{p_c(T_0)}{p_T(T)} = \gamma^{TY}\sqrt{ln\left(\frac{T}{T_0}\right)} + 1 \quad (20)$$

where $p_c(T_0)$ is the preconsolidation pressure at room temperature, $p_T(T)$ is the thermal yield limit at temperature T and γ^{TY} is an evolution parameter depending on the soil type.

At stresses below the thermal yield limit, the soil will behave elastically exhibiting thermal expansive behavior. When the stresses exceed the thermal yield limit due to mechanical loading, thermal loading or a combination of both, thermo-plastic strains will be generated with thermal hardening or increase in the thermal yield limit. Expansive and/or compressive behavior can be observed in this region between the thermal yield limit and the loading yield limit. As the stresses continue to increase beyond the loading yield limit, plastic strains will be generated due to the hardening of both the thermal and the loading yield limits. Only compressive behavior will be observed beyond the loading yield limit. This behavior depicted in the model proposed by Abuel-Naga, Bergado, Bouazza, & Ramana (2007) agrees with the past research where reversible expansion and irreversible contraction were observed in OC clays and NC clays respectively (Robinet, Rahbaoui, Plas, & Lebon, 1996; Abuel-Naga, Bergado, & Chaiprakaikeow, 2006).

The above model by Abuel-Naga, Bergado, Bouazza, & Ramana (2007) considers both elastic and plastic components of volumetric strain due to thermal and mechanical loading. The elastic component of volumetric strain due to mechanical and thermal loading is expressed using the classical Cam-clay model and thermal expansive behavior respectively, as shown in equation 21.

$$d\varepsilon_v^e = \left(\frac{\kappa}{1+e_0}\right)\frac{dp'}{p'} + \alpha dT \quad (21)$$

where κ is the slope of the swelling line on a e vs $\ln p'$ plot, e_0 is the initial void ratio and α is the drained volumetric thermal expansion coefficient of soil. The plastic component of the volumetric strain is given as follows.

$$d\varepsilon_v^p = \frac{1}{1+e_0}\left\{[\lambda - (\kappa + \omega_T)]\frac{dp_c}{p_c} + \omega_T \frac{dp_T}{p_T}\right\} \quad (22)$$

where λ is the slope of the compression line on a e vs $\ln p'$ plot and ω_T is the plastic hardening modulus of the thermal yield limit respectively.

The effective stress p' was obtained by deducting the pore pressure p obtained using the Navier stokes equations from the total stress. Total stresses depend on the vertical elevation and the surcharge applied. ω_T is expressed by equation 23.

$$\omega_T = \frac{(\lambda-\kappa)ln[p_c(T_0)/p_c(T)]}{\ln[p_c(T_0)/p_T(T)]} \quad (23)$$

In the model proposed by Abuel-Naga, Bergado, Bouazza, & Ramana (2007) ω_T is obtained using a secant approach. However, in consideration of the plastic behavior of the soil in the thermoelasto-plastic region, a more appropriate tangential ω_T (Gunaratne, M., Personal Communication) was used in this numerical model as in equation 24.

$$\omega_T = \frac{(\lambda-\kappa)ln[p_c(T)/p_c(T+\Delta T)]}{\ln[p_T(T)/p_T(T+\Delta T)]} \quad (24)$$

The experimental results of Abuel-Naga, Bergado, Bouazza, & Ramana (2007) also show that the preconsolidation pressure is independent of temperature during heating but increases during cooling. On the other hand, the preconsolidation pressure at constant plastic strain decreases with a temperature increment and is obtained using the relationship proposed by Laloui & Cekerevac (2003) as follows.

$$\frac{p_c(T)}{p_c(T_0)} = 1 - \gamma^{LY} log\left(\frac{T}{T_0}\right) \quad (25)$$

where γ^{LY} is another model parameter depending on the soil type.

The consolidation curves for the room temperature T_0 and an elevated temperature T are shown in Figure 2.2, where p_T is the thermal yield limit and p_c is the loading yield limit. The expansive behavior at stresses below p_T, expansive-contractive behavior at stresses between p_T and p_c and contractive behavior at stresses beyond p_c can be observed in the consolidation curve at T when comparing with that of T_0. It is also illustrated at load p_c, how a settlement increment Δ is obtained only due to a temperature increase from T_0 to T.

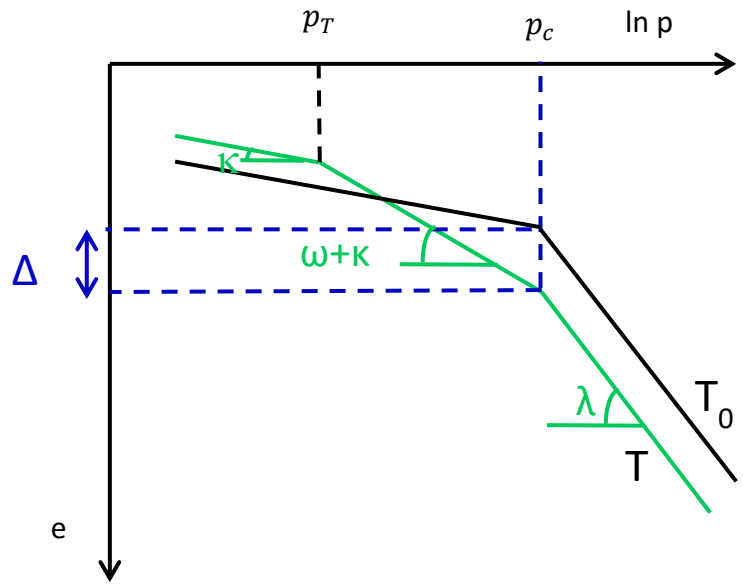

Figure 2.2 Consolidation curves for temperatures T_0 and T

2.3 Modeling the Temperature Distribution in the Soil

The transient temperature distribution through the soil was modeled using the Fourier's equation of heat transfer (Bergman, Lavine, Incropera, & Dewitt, 2007). When a soil mass is

heated by a heat source in a vertical drain, a temperature regime will be created in the surrounding area. This temperature distribution will determine the $\partial T/\partial t$ to be used in equation 14 to obtain the corresponding thermal expansion. In this research, a simple model is proposed to determine the temperature distribution around a heat source.

Consider a cylindrical soil mass with a heat source along its central axis. Heat from the source will be transferred through the soil medium by conduction. The temperature at different radial locations will gradually increase with time until the steady state temperatures are reached. The heat transfer equation (equation 26) was used to model the temperature distribution along a radius assuming no heat loss to the atmosphere.

$$\frac{\partial^2 T}{\partial r^2} + \frac{1}{r}\frac{\partial T}{\partial r} = \frac{\rho_s C}{k}\frac{\partial T}{\partial t} \tag{26}$$

where ρ_s is the density of the soil, C is the specific heat capacity of the soil and k is the thermal conductivity of the soil. The cooling law was used to obtain the temperatures when the soil is cooled after removal of the heat source.

$$\frac{dT}{dt} = -\frac{hA}{\rho_s C}(T(t) - T_0) \tag{27}$$

where h is the convective heat transfer coefficient and A is the surface area.

2.4 Computer Coding

The heat equation (26), continuity equation (14), momentum equation (19) and the soil compressibility relationships (21 & 22) were solved in the numerical model to obtain the temperatures, porosities, velocities and pressures respectively at different locations. The differential equations governing the fluid flow and heat transfer were programmed on the computer using the finite difference method based on a forward time centered space scheme.

Owing to the axisymmetric nature of the soil domain and uniformity of temperature in the vertical direction, a radial axis in any horizontal plane can be considered in the one dimensional model.

In the numerical model, radii were divided into elements and nodes were introduced at the center (odd nodes) and boundaries (even nodes) of each element as seen in Figure 2.3. The porosity values obtained from the continuity equation and the pressures obtained using the compressibility relationships were calculated at odd nodes while the velocities obtained from the momentum equation were calculated at the even nodes. On the other hand, temperatures were calculated at both odd and even nodes.

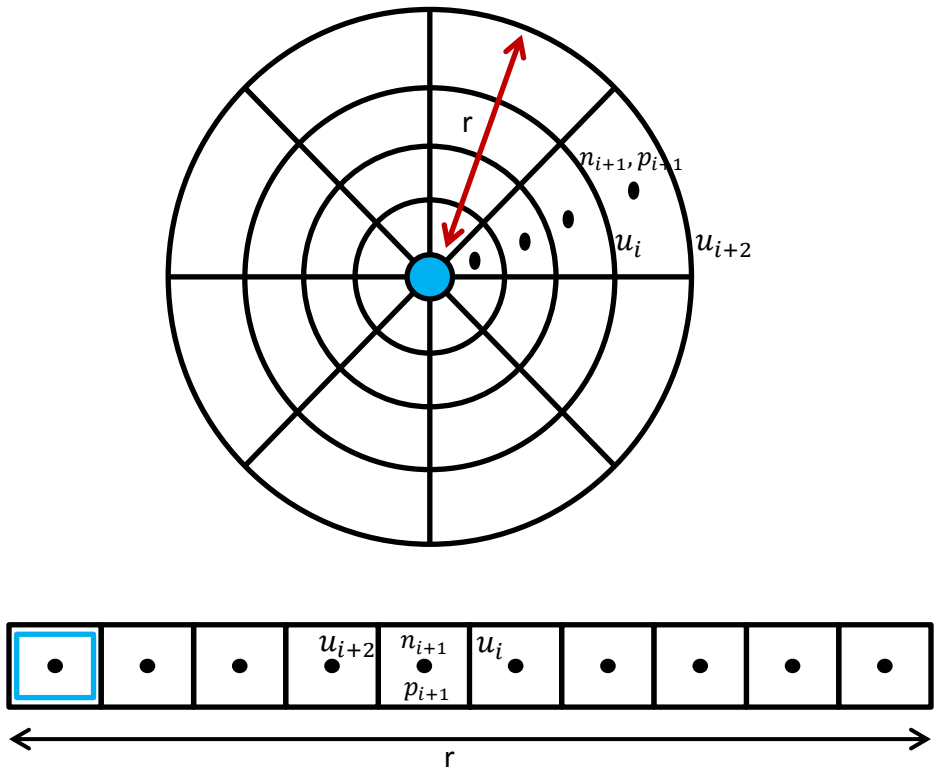

Figure 2.3 Arrangement of elements and nodes along a radius

2.4.1 Finite Difference Approximations

The finite difference approximations for the heat, continuity and momentum equations are shown in equations 28, 29 and 30 respectively.

$$\frac{T_{i+3}^t - 2T_{i+1}^t + T_{i-1}^t}{(\Delta r)^2} + \frac{1}{r_{i+1}} \frac{(T_{i+3}^t - T_{i-1}^t)}{2\Delta r} = \frac{\rho C}{k} \frac{(T_{i+1}^{t+1} - T_{i+1}^t)}{\Delta t} \tag{28}$$

$$-n_{i+1}^t \frac{(u_{i+2}^t - u_i^t)}{\Delta r} - \left(\frac{u_{i+2}^t + u_i^t}{2}\right) \frac{(n_{i+3}^t - n_{i-1}^t)}{2\Delta r} - \frac{n_{i+1}^t \left(\frac{u_{i+2}^t + u_i^t}{2}\right)}{r_{i+1}} = \frac{(n_{i+1}^{t+1} - n_{i+1}^t)}{\Delta t} + n_{i+1}^t \beta \frac{(T_{i+1}^{t+1} - T_{i+1}^t)}{\Delta t} \tag{29}$$

$$\frac{\mu}{\rho}\left[\frac{(\frac{n_{i+1}^t + n_{i-1}^t}{2})(u_{i+2}^t - 2u_i^t + u_{i-2}^t)}{\Delta r^2} + \frac{(\frac{n_{i+1}^t + n_{i-1}^t}{2})(u_{i+2}^t - u_{i-2}^t)}{r_i 2\Delta r} - \frac{(\frac{n_{i+1}^t + n_{i-1}^t}{2})u_i^t}{{r_i}^2}\right] - \frac{(\frac{n_{i+1}^t + n_{i-1}^t}{2})}{\rho} \frac{(p_{i+1}^t - p_{i-1}^t)}{\Delta r} -$$

$$\frac{150\mu}{\rho}\left(\frac{1 - (\frac{n_{i+1}^t + n_{i-1}^t}{2})}{\frac{n_{i+1}^t + n_{i-1}^t}{2}}\right)^2 \frac{1}{{d_p}^2} u_i^{t+1} = \frac{(\frac{n_{i+1}^t + n_{i-1}^t}{2})(u_i^{t+1} - u_i^t)}{\Delta t} \tag{30}$$

A central difference scheme with 2nd order accuracy was used in the spatial domain. Forward and backward difference schemes with the same accuracy were used at the boundaries. The finite difference coefficients for different schemes are given in Table 2.1 – Table 2.3.

Table 2.1 Coefficients for central difference scheme

Derivative	**Coefficients**			**Error**
	-1	**0**	**1**	
1	-1/2	0	½	$O(h^2)$
2	1	-2	1	$O(h^2)$

Table 2.2 Coefficients for forward difference scheme

Derivative	**Coefficients**				**Error**
	0	**1**	**2**	**3**	
1	-1	1			O(h)
1	-3/2	2	-1/2		$O(h^2)$
2	1	-2	1		O(h)
	2	-5	4	-1	$O(h^2)$

Table 2.3 Coefficients for backward difference scheme

Derivative	**Coefficients**				**Error**
	-3	**-2**	**-1**	**0**	
1			-1	1	O(h)
		1/2	-2	3/2	$O(h^2)$
2		1	-2	1	O(h)
	-1	4	-5	2	$O(h^2)$

2.5 Boundary and Initial Conditions

Reasonable assumptions were made regarding the boundary and initial conditions of the numerical model. An influence area in the soil around the vertical drain was considered and the radial velocity of flow at the edge of the influence zone was considered to be zero. The pressure in the drain was maintained at hydrostatic pressure. The temperature at the drain was maintained at the specific maximum temperature induced by the source used for thermal

treatment and a 1m influence radius was assumed based on literature (Pothiraksanon, Bergado, & Abuel-Naga, 2010). The initial velocities were considered to be zero and the initial temperature in the entire domain was assumed to be the ambient temperature T_0. An initial porosity for the soil can be specified while the water pressures and total stresses depend on the vertical elevation and the surcharge. The flow chart for the numerical model is presented in Figure 2.4.

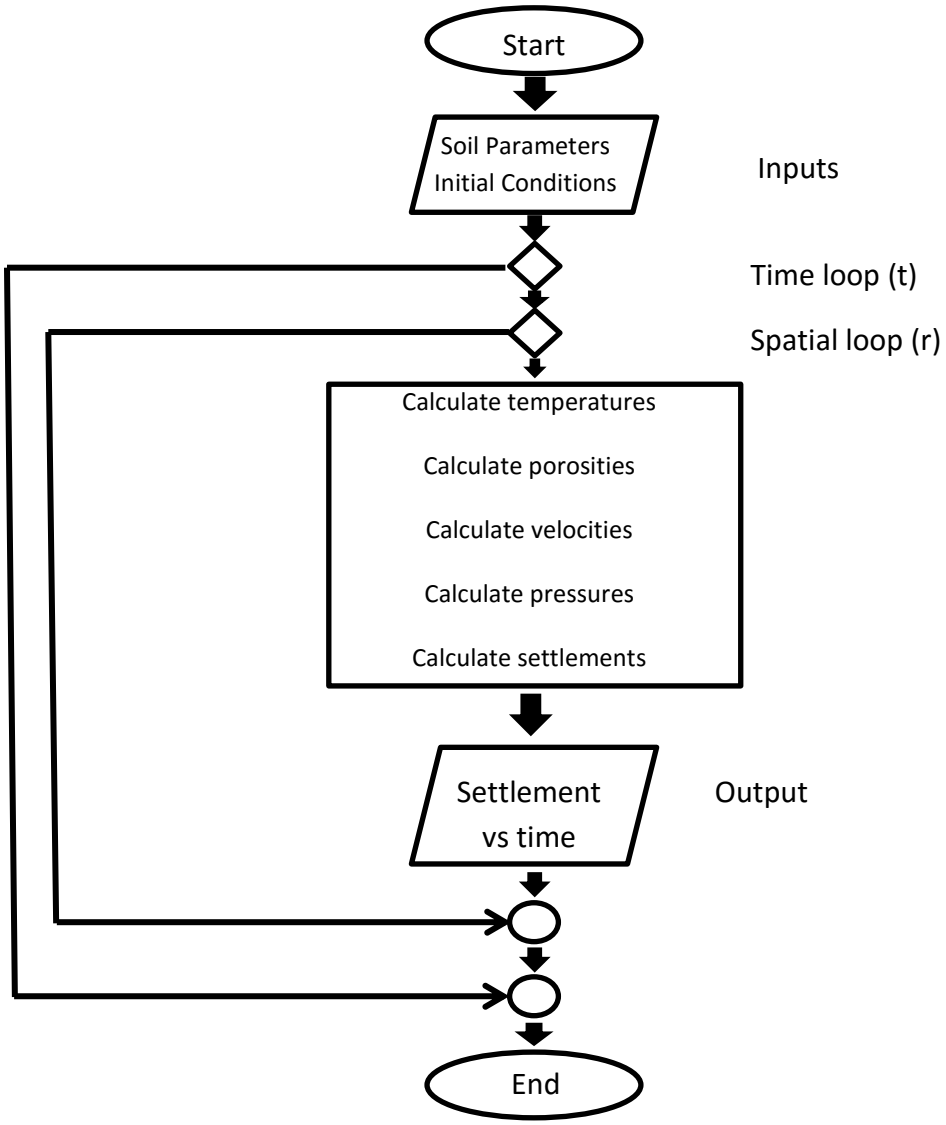

Figure 2.4 Flow chart for the numerical model

CHAPTER 3: VERIFICATION OF PROGRAM RESULTS

The developed numerical program is capable of modeling the consolidation process for OC and NC clays. The program outputs mainly consist of settlement vs time data for locations along a radius. Although this is the main output investigated in this research, it is also possible to obtain other parameters such as pore pressure variations, flow velocities and effective stress variations along radial locations. Before investigating the consolidation behavior under a thermal treatment, the accuracy of program output results was first checked. The results were checked for the two scenarios where the soil is consolidated with and without thermal treatment.

3.1 Radial Consolidation without Thermal Treatment

The first check was to verify if the program provided accurate results for typical radial consolidation under a surcharge. A clay sample of 0.45m diameter and 0.7m height under a 50kPa surcharge was considered for this purpose. The assumed properties of clay are given in Table 3.1.

The results obtained from the program were checked with the solution for radial consolidation of a soil mass, developed by Barron (1948) as shown in equation 31.

$$\frac{\partial u}{\partial t} = C_h \left[\frac{1}{r}\frac{\partial u}{\partial r} + \frac{\partial^2 u}{\partial r^2}\right] \tag{31}$$

where u is the excess pore water pressure at time t and C_h is the horizontal coefficient of consolidation of the soil. The average degree of consolidation $U_h$is expressed in equation 32.

$$U_h = 1 - \exp\left(\frac{-8T_h}{\mu}\right) \quad (32)$$

$$T_h = \frac{C_h t}{D^2} \quad (33)$$

$$\mu = \frac{n^2}{n^2-1}\ln(n) - \frac{3n^2-1}{4n^2} \quad (34)$$

where D is the diameter of the equivalent soil cylinder, d is the equivalent diameter of the drain and $n = D/d$. The above solution neglects the smear zone around the soil cylinder.

Table 3.1 Clay properties used in the program for radial consolidation without thermal treatment

Total unit weight	14.7 kN/m3
Initial porosity	0.67
Pre-consolidation pressure	50kPa
κ	0.1
λ	0.59

The program results were in agreement with the results obtained using equations 31-34 for horizontal consolidation for a C_h value of 3m^2/year. Laboratory experiments performed by Artidteang, Bergado, Saowapakpiboon, Teerachaikulpanich, & Kumar (2011) for a reconstituted clay sample of similar dimensions, unit weight and pre-consolidation pressure (Table 3.1)

subjected to a 50kPa surcharge, reported a C_h value of 1.93m^2/year. Program results and the predicted results from the solution are shown in Figure 3.1.

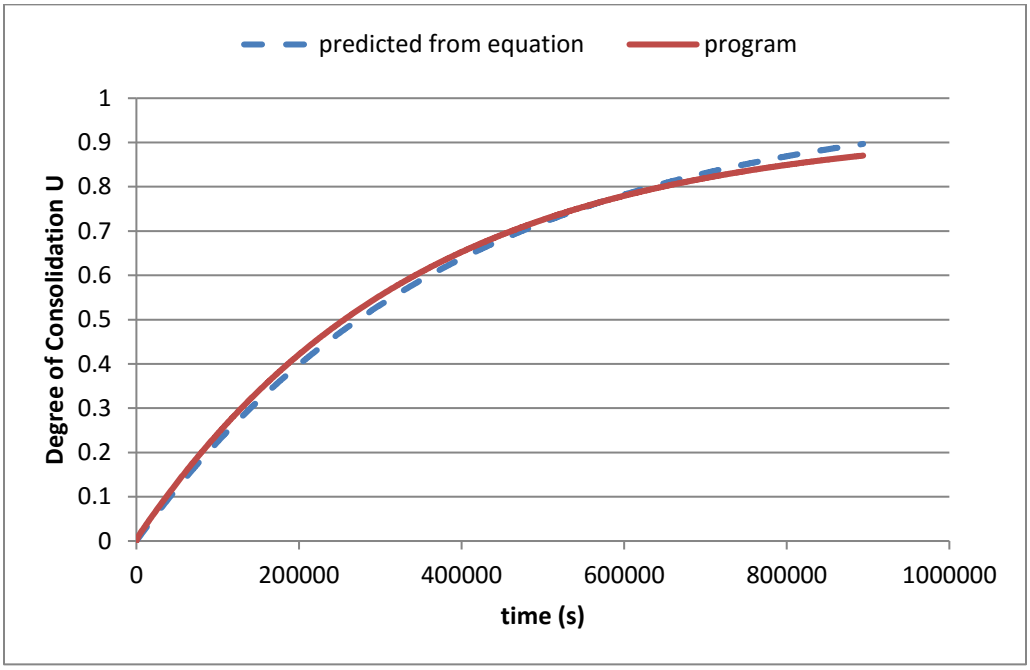

Figure 3.1 Comparison of program results and results predicted using equations for degree of consolidation

3.2 Radial Consolidation with Thermal Treatment

As discussed in section 1.3 it has been conclusively stated in many studies (Robinet, Rahbaoui, Plas, & Lebon, 1996; Abuel-Naga, Bergado, Bouazza, & Ramana, 2007) that volume changes in clays due to heating is stress history dependent where highly OC clays exhibit expansive behavior and NC clays exhibit contractive behavior. As the over consolidation ratio (OCR) reduces, the expansive behavior gradually decreases and the clay starts to contract. The proposed model by Abuel-Naga, Bergado, Bouazza, & Ramana (2007) incorporates the above

behavior appropriately. If the stress path is completely inside the thermal yield limit (p_T), the soil behavior will be completely expansive whereas if it is outside p_T it would be contractive. If a stress path extends from the elastic region to the plastic region straddling the thermal yield limit, the soil will exhibit combined expansive-contractive behavior. This behavior can also be observed clearly from the program results as seen in Figure 3.2.

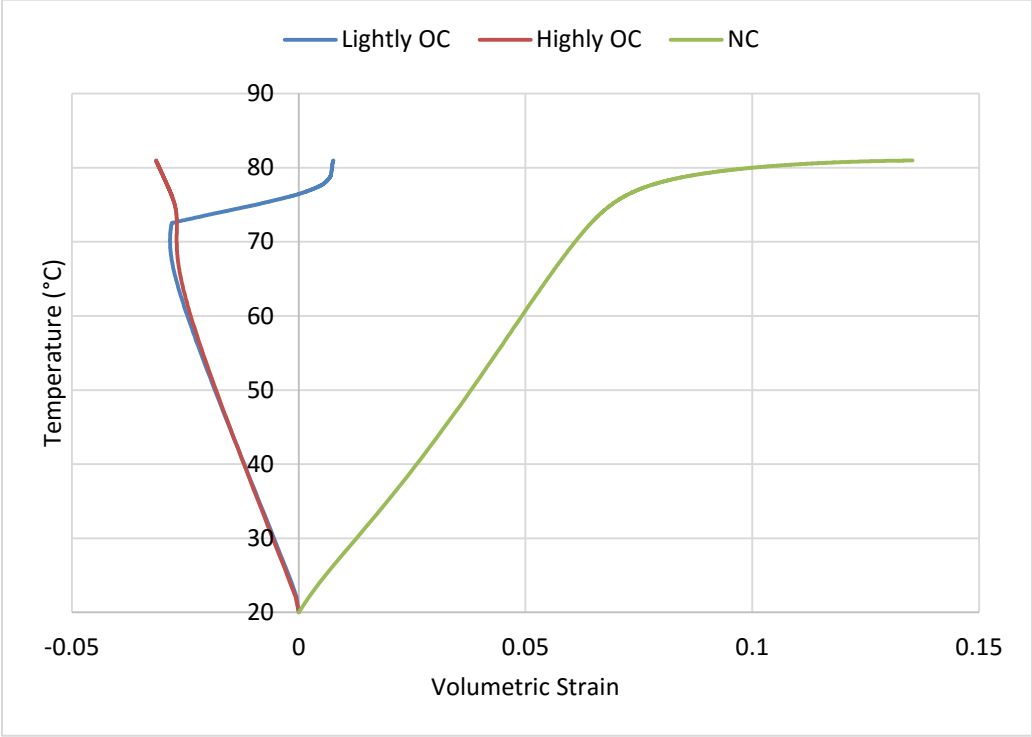

Figure 3.2 Behavior of NC, highly OC and lightly OC clays upon heating

To check the performance of the program for consolidation coupled with thermal treatment, settlements were observed with and without a temperature increment under the same soil conditions. The clay sample was of 0.45m diameter and 0.7m height and was subjected to a 50kPa surcharge. The maximum temperature at the heat source was 90°C. The assumed soil properties are given in Table 3.2.

Table 3.2 Clay properties used in the program for radial consolidation with thermal treatment

Total unit weight	14.7 kN/m3
Initial porosity	0.67
Pre-consolidation pressure	50kPa
κ	0.1
λ	0.59
γ^{TY}	1.1
γ^{LY}	0.43
α	0.0007

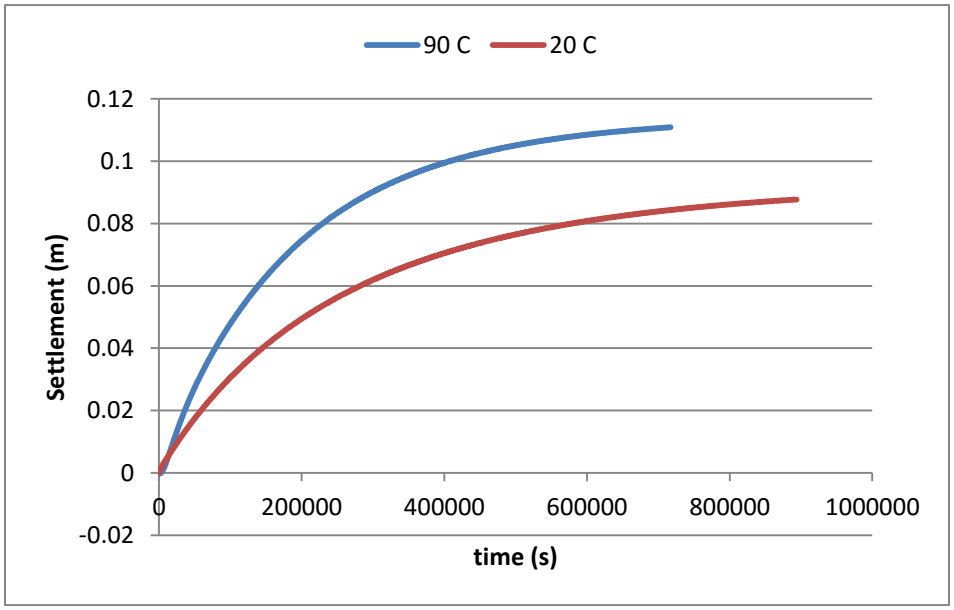

Figure 3.3 Settlement curves at 20˚C and 90˚C

Based on Figure 3.3, a 26.45% increase in the final settlement can be observed when subjected to a thermal treatment from 20°C to 90°C. Laboratory experiments performed by

Artidteang, Bergado, Saowapakpiboon, Teerachaikulpanich, & Kumar (2011) under similar loading conditions for a sample of similar dimensions, unit weight and pre-consolidation pressure (Table 3.2) report a 25% increase in the final settlement for a reconstituted clay specimen. As discussed in Chapter 1, an increase in the rate of settlement and the magnitude can be observed from the program results in Figure 3.3.

CHAPTER 4: RESULTS AND DISCUSSION

The numerical program was used to observe the effect of temperature on the consolidation behavior of the soil. Multiple cases were run varying the temperature of the heat source, surcharge load and the initial porosity of NC clay. First, the variations in pore pressures in the soil and flow velocities were investigated. Then the effect on settlement due to varying surcharge loads, temperature increments and initial void porosities were observed. The behavior of NC clays at elevated temperatures and the effect on settlement during cooling are also discussed in this chapter.

4.1 Variation of Flow Velocity and Pore Pressure with Temperature

As discussed in Chapter 3, an increase in the rate of settlement as well as its magnitude could be observed when the soil is subject to a thermal treatment. Furthermore, the behavior of the flow velocities and pore pressures were observed for a soil subjected to a 100 kPa surcharge. Two cases were run at the ambient temperature (20°C) and at 90°C respectively. As expected, an increase in pore pressures can be seen initially due to the increase in temperature. However, due to higher dissipation rates under drained conditions, the pore pressures dissipates faster over time compared to the case without a temperature increment, as shown in Figure 4.1. Figure 4.2 compares the flow velocities for the two cases and an increase in the flow

velocity can be observed at the elevated temperature. This can be attributed to the reduction in viscosity corresponding to an increase in temperature.

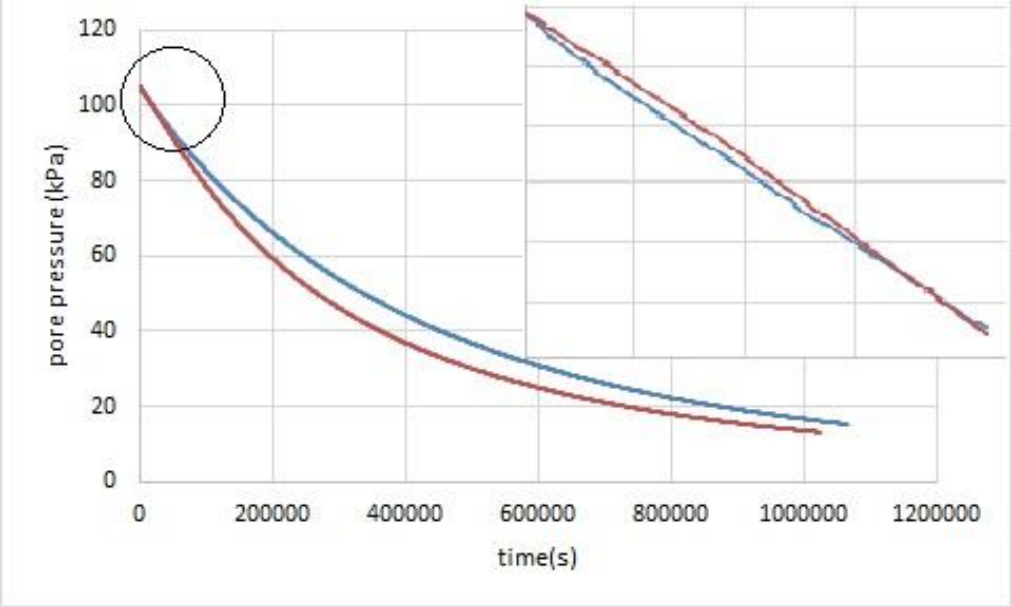

Figure 4.1 Pore pressure variation for 20°C and 90°C

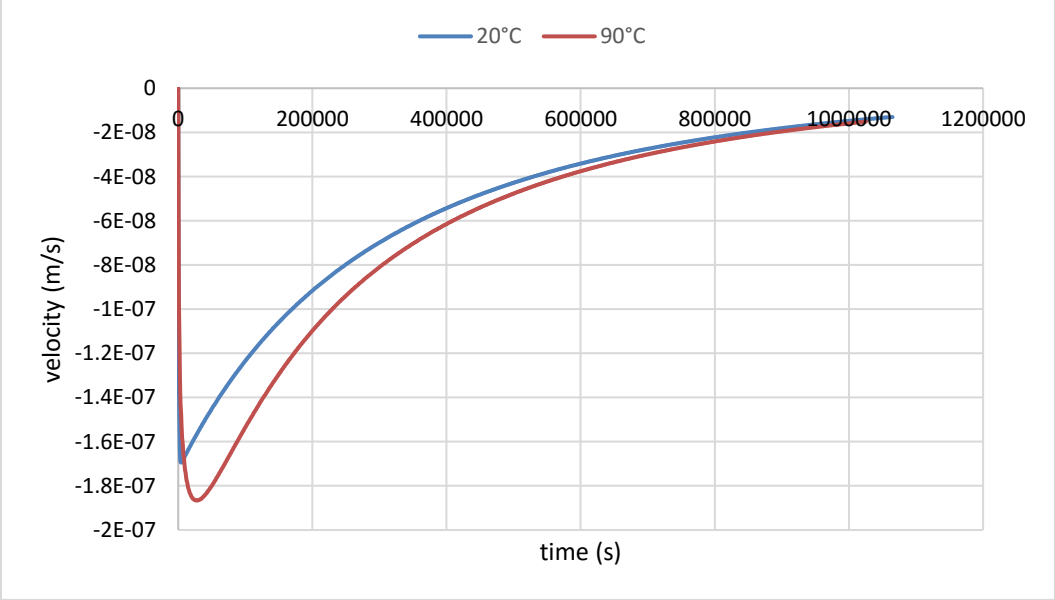

Figure 4.2 Velocity variation for 20°C and 90°C

4.2 Increase in Settlement

To investigate the effect of temperature on the ultimate final settlement, multiple cases were run varying the temperature increments and surcharge loads ranging from 50 kPa to 200 kPa. The maximum settlement (s_{max}) at elevated temperatures was compared with the settlement (s_0) at the ambient temperature.

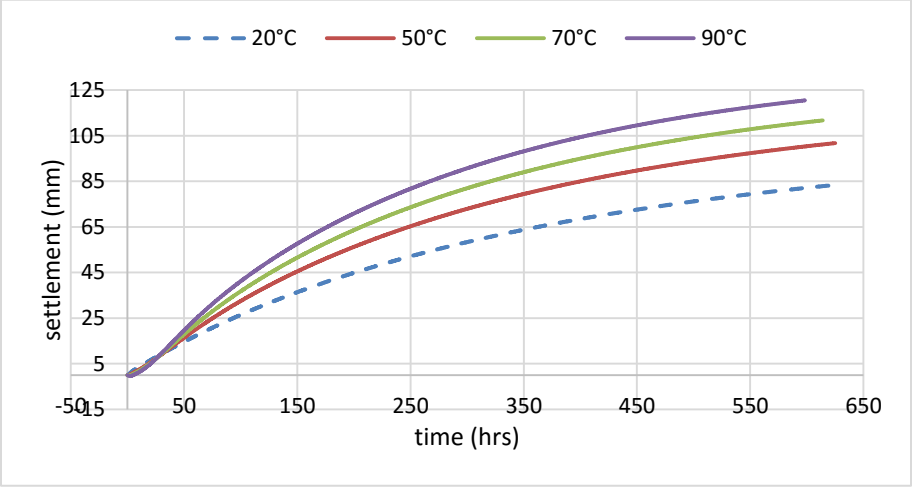

Figure 4.3 Settlement history at different temperatures for a 50 kPa surcharge

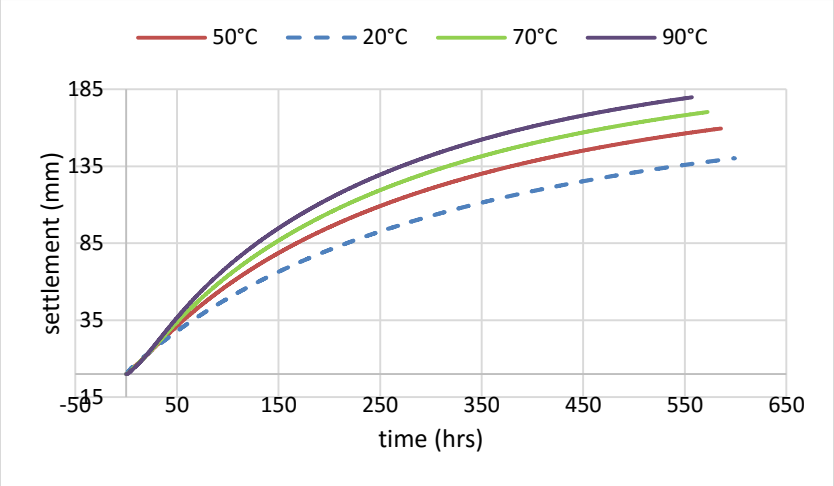

Figure 4.4 Settlement history at different temperatures for a 100 kPa surcharge

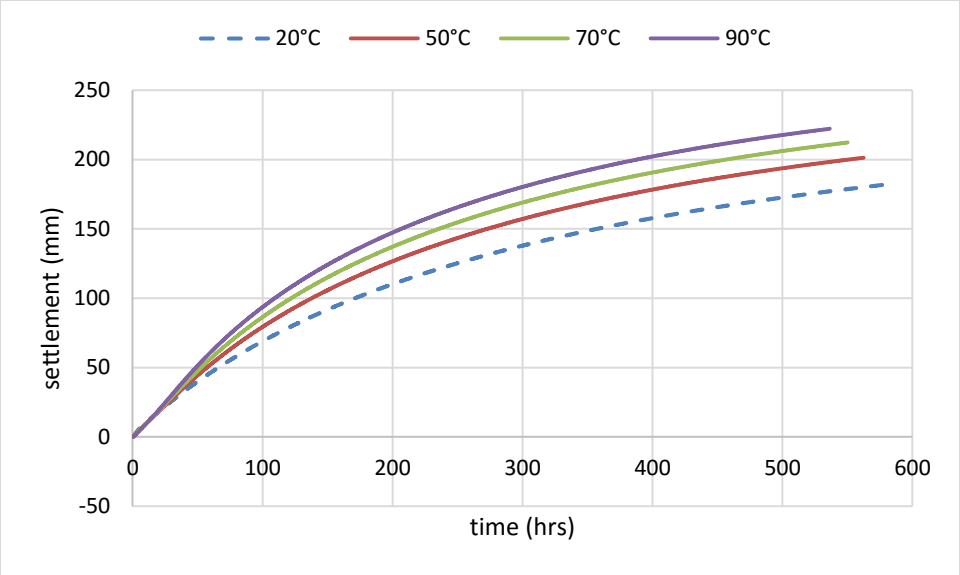

Figure 4.5 Settlement history at different temperatures for a 150 kPa surcharge

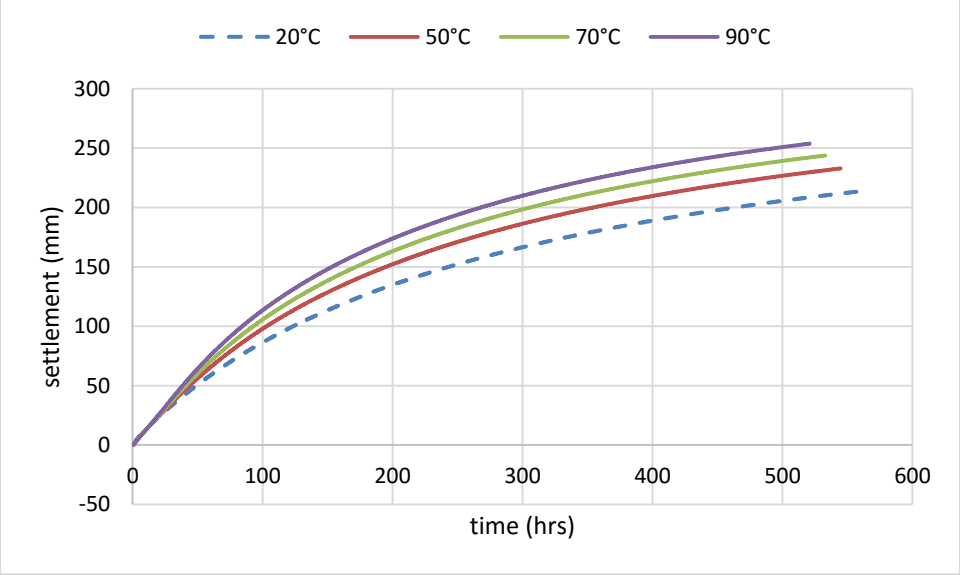

Figure 4.6 Settlement history at different temperatures for a 200 kPa surcharge

It can be observed from the results in Figures 4.3 – 4.6 that for a given surcharge, the magnitude of the final settlement increases as the maximum temperature at the source increases. However, the effect of temperature on the settlement reduces as the surcharge

increases. Therefore, the maximum effect from a thermal treatment can be utilized at relatively lower surcharge levels. This complements the coupled thermal and mechanical load induced consolidation process, as a lower surcharge load could be used whilst obtaining the maximum output of the thermal treatment. The results are summarized in Figure 4.7.

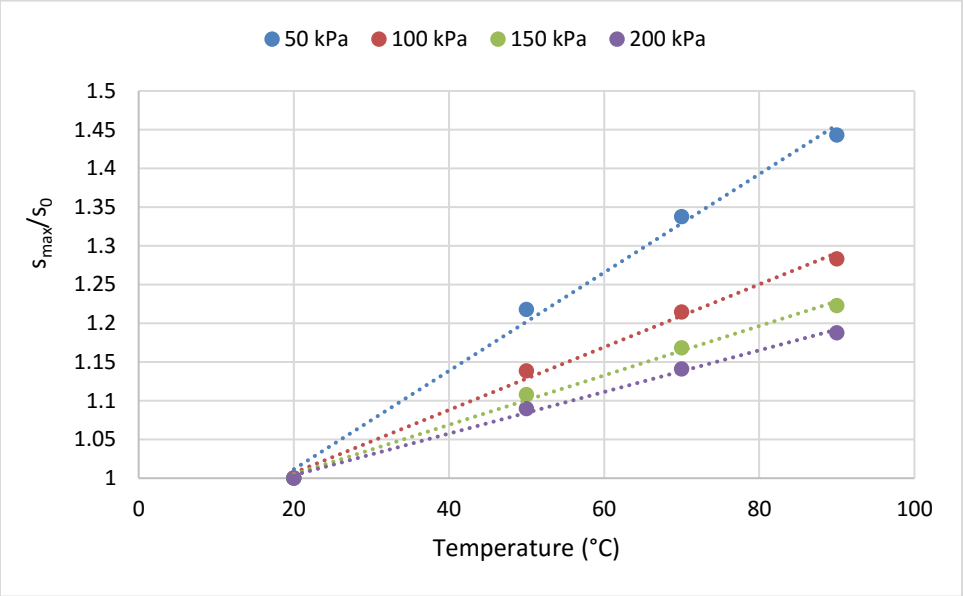

Figure 4.7 Effect of temperature and surcharge on settlement

The time rate of settlement also reduces as the temperature increases for a given surcharge as shown in Figure 4.8 where time taken for 90% consolidation at different maximum temperatures was compared. The reduction in the time rate on the other hand, decreases with an increase in surcharge. However, it should be noted that the time taken for 90% consolidation (t_{90}) at elevated temperatures and the time taken for 90% consolidation at the ambient temperature (t_0) correspond to different magnitudes of settlement. A better comparison would be to relate the time taken to reach a specific magnitude of settlement at different temperatures. Let the time taken for 90% consolidation at ambient temperature

(20°C) be t_0 and the corresponding magnitude of settlement be s_{90}. The time t' taken to reach a settlement of s_{90} at different elevated temperatures was compared with t_0. As seen in Figure 4.9, a significant reduction in the time can be observed as the temperature increases and this effect reduces as the surcharge is increased.

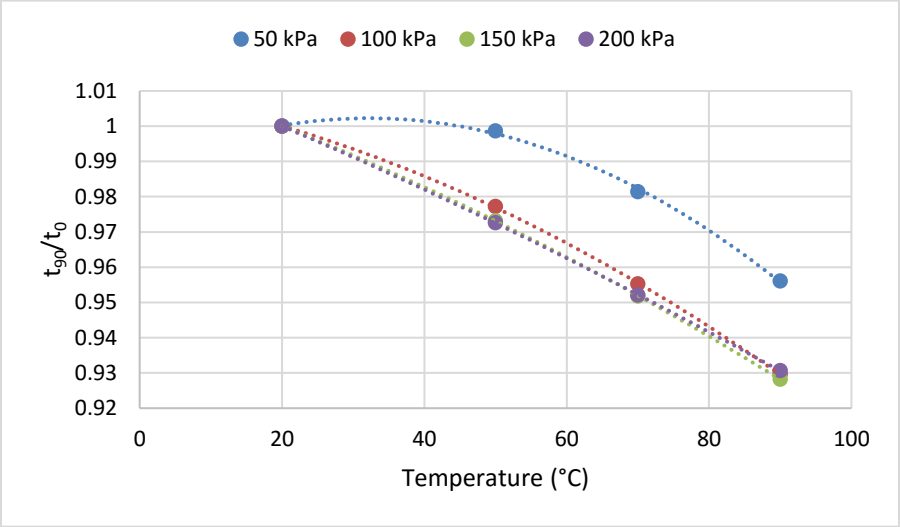

Figure 4.8 Effect of temperature and surcharge on time for 90% consolidation

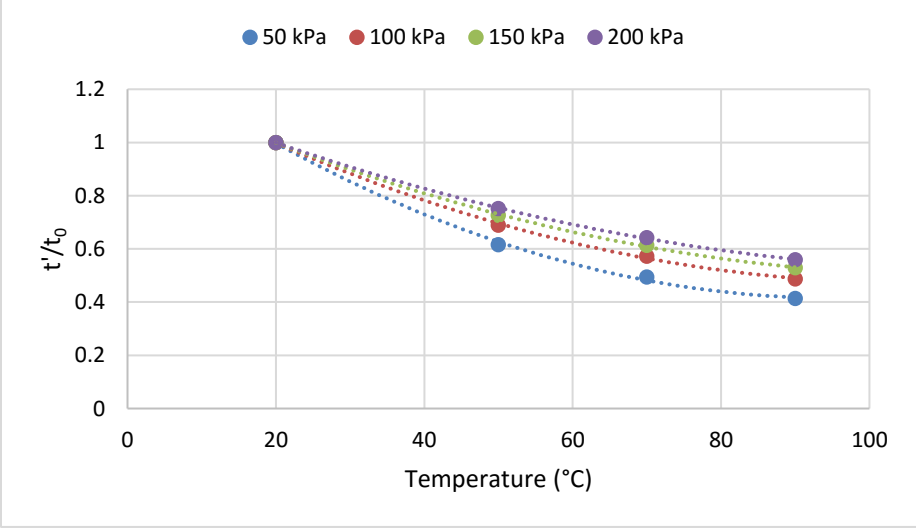

Figure 4.9 Effect of temperature and surcharge on time to reach s_{90}

Based on the above results it can be concluded that the magnitude and rate of settlement increases as the maximum temperature of the heat source increases. However, this increase is less at higher surcharge loads.

4.3 Effect from Initial Void Ratio

The coefficient of consolidation (C_v) is dependent on the permeability of the soil (k), the density of water (ρ) and the coefficient of volume compressibility (m_v) as shown in equation 35.

$$C_v = \frac{k}{\rho m_v} \tag{35}$$

$$m_v = \frac{a_v}{1+e_0} \tag{36}$$

where a_v is the coefficient of compressibility and e_0 is the initial void ratio.

The coefficient of compressibility describes the relationship between an increase in effective stress and the corresponding change in the void ratio. Therefore, based on the above relationships, permeability, density of water, surcharge and the initial void ratio are the factors that would have an effect on consolidation. The permeability can also be related to the void ratio by the following relationship (Carrier, 2003).

$$k = \frac{\rho}{\mu}\frac{1}{C_{K-C}}\frac{1}{{S_0}^2}\frac{e^3}{(1+e)} \tag{37}$$

The void ratio can be related to the porosity by the following equation.

$$e = \frac{n}{1-n} \tag{38}$$

The effect of surcharge has been investigated in section 4.2. To consider the effect of the initial porosity, multiple cases were run varying the initial porosity at different surcharges and temperatures. The results are presented in Figures 4.10 to 4.13.

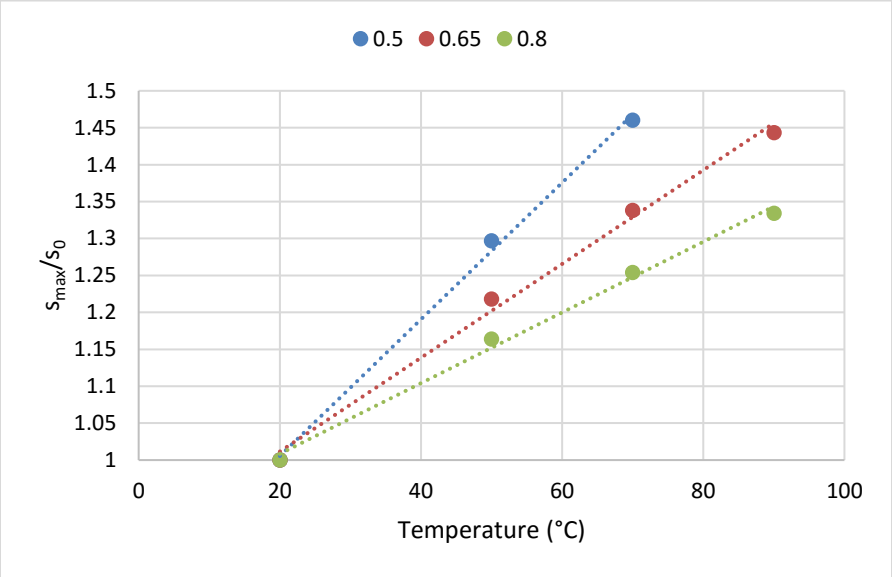

Figure 4.10 Effect of temperature and initial porosity on settlement at 50 kPa

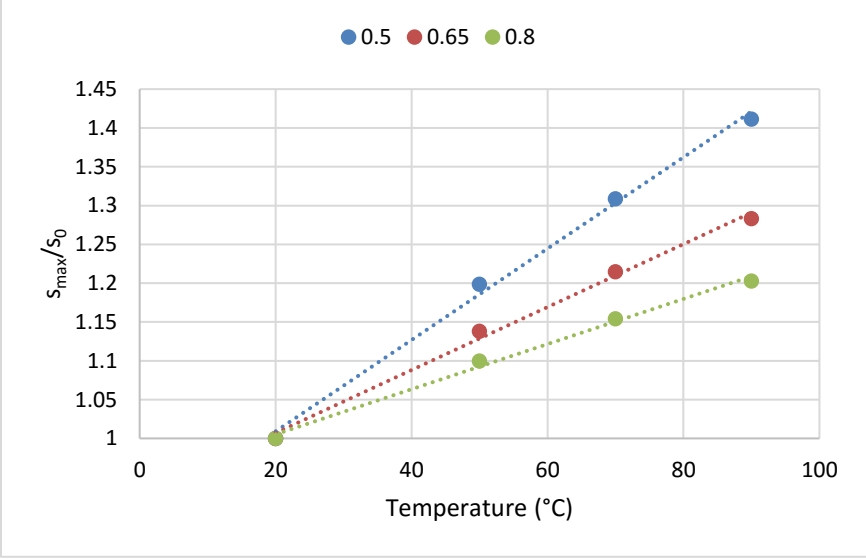

Figure 4.11 Effect of temperature and initial porosity on settlement at 100 kPa

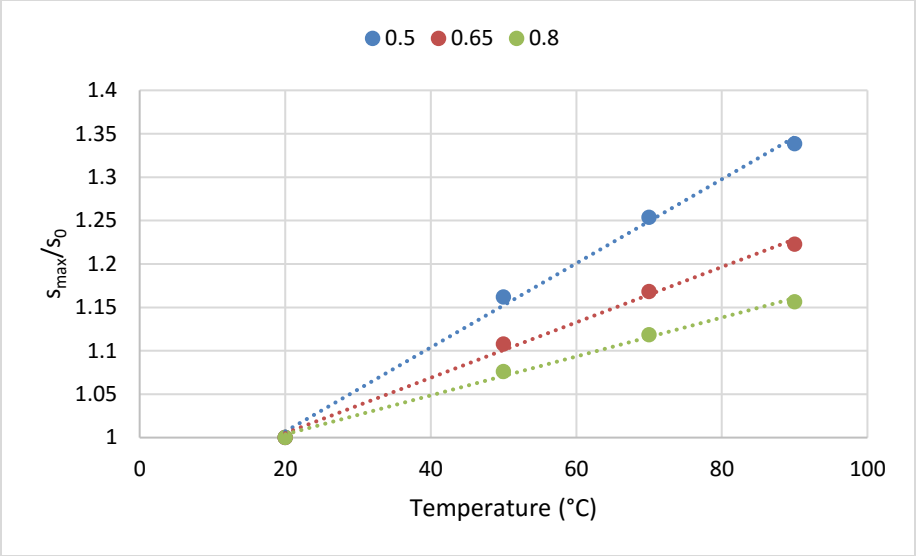

Figure 4.12 Effect of temperature and initial porosity on settlement at 150 kPa

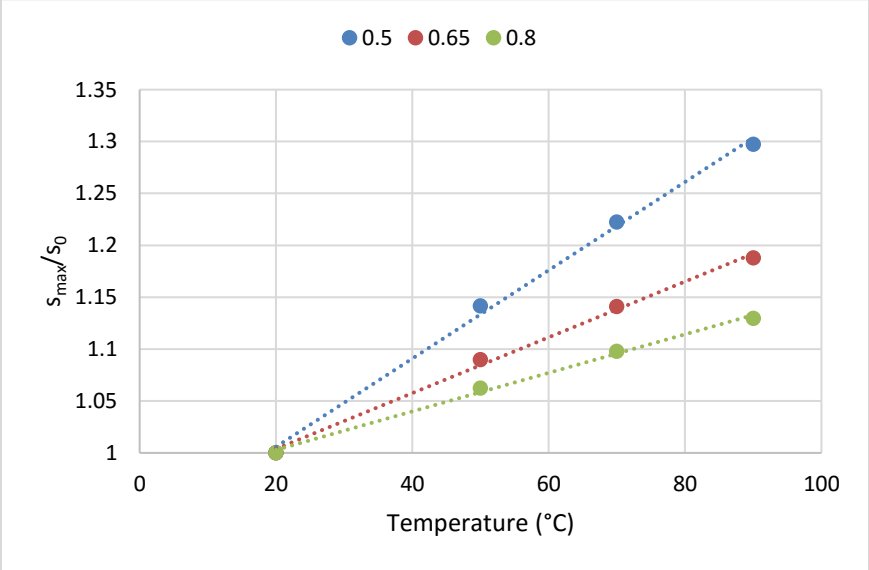

Figure 4.13 Effect of temperature and initial porosity on settlement at 200 kPa

It can be observed that the effect of temperature on the settlement is greater at lower initial porosities. Similarly, the effect on the time to reach a specified settlement (s_{90}) at different initial porosities can be observed as well. It can be seen from Figures 4.14 – 4.17 that

the time to reach a specified settlement s_{90} decreases as the initial porosity increases. However the effect of the initial porosity is insignificant at higher surcharge loads.

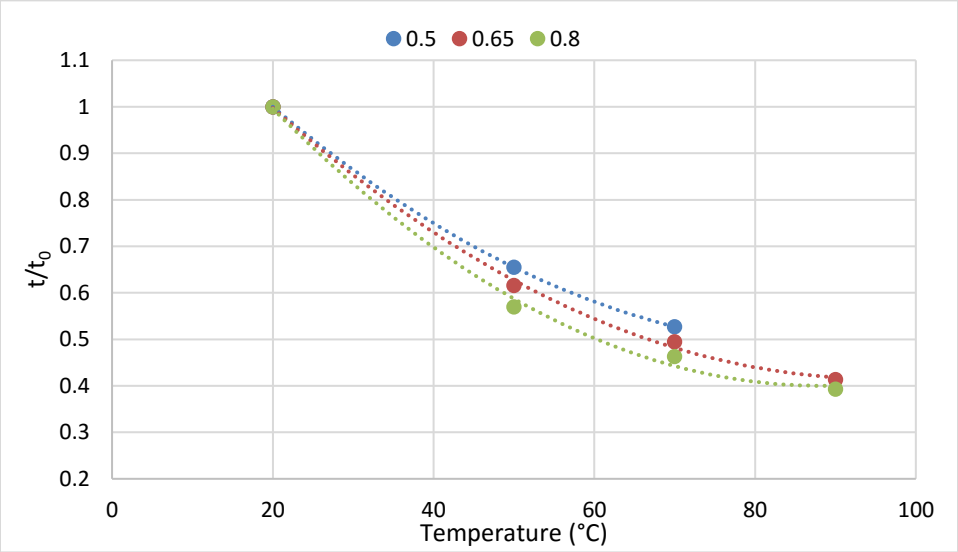

Figure 4.14 Effect of temperature and initial porosity on time to reach s_{90} at 50 kPa

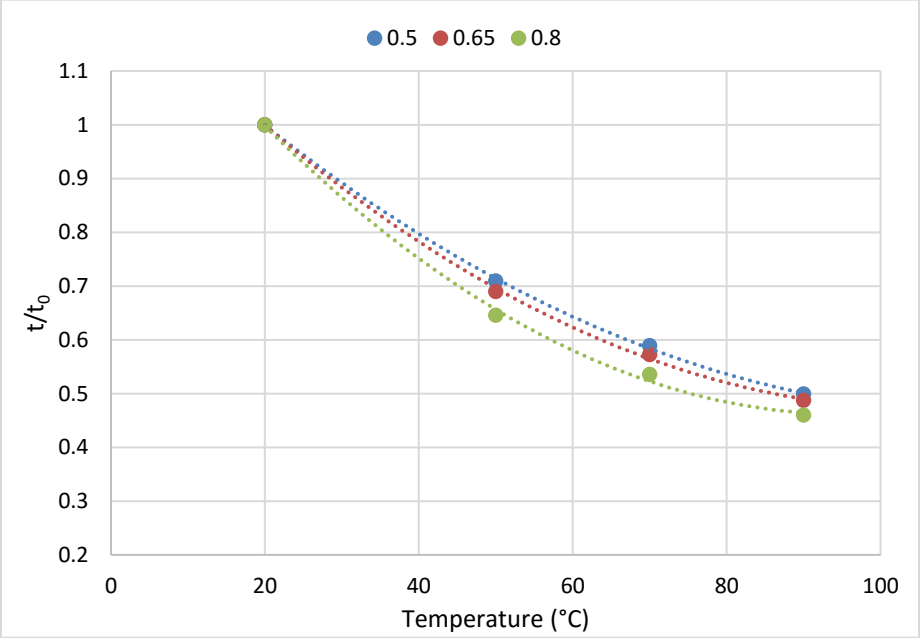

Figure 4.15 Effect of temperature and initial porosity on time to reach s_{90} at 100 kPa

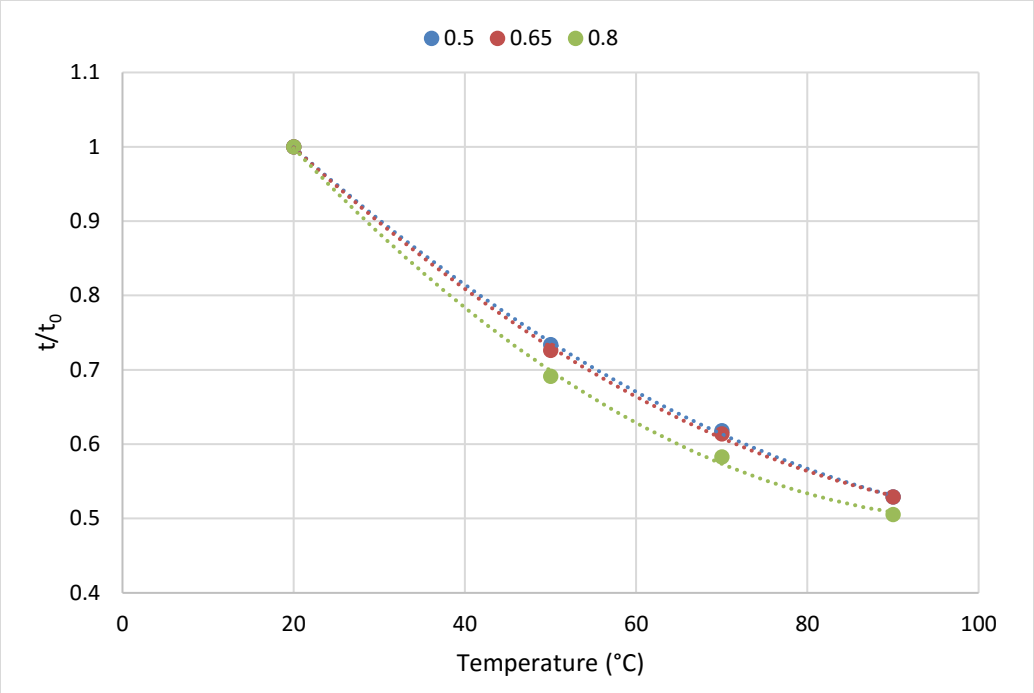

Figure 4.16 Effect of temperature and initial porosity on time to reach s_{90} at 150 kPa

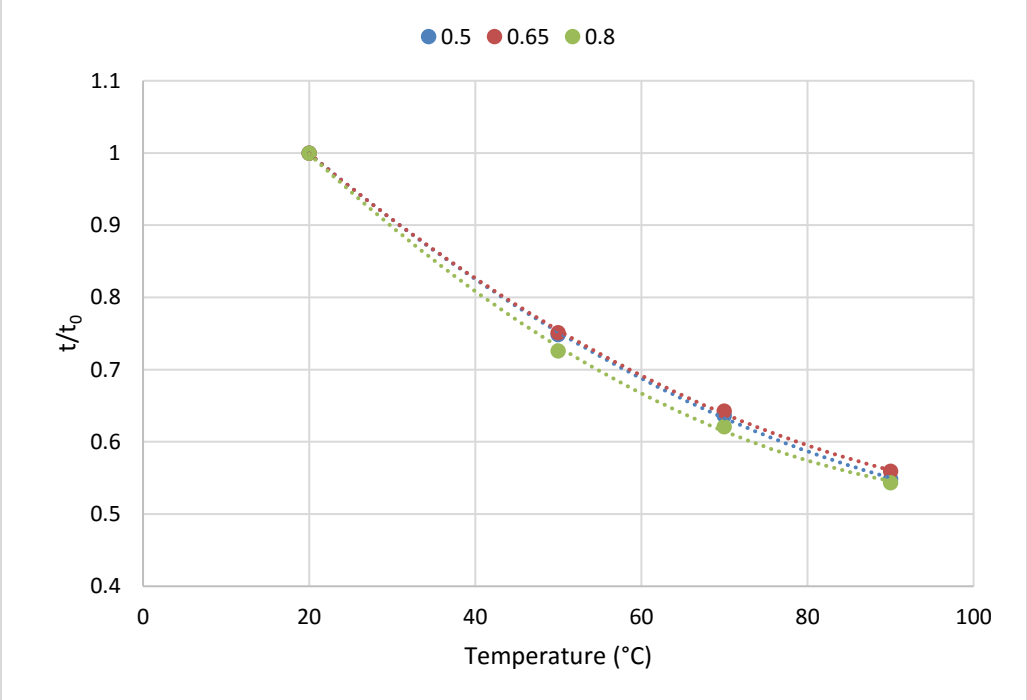

Figure 4.17 Effect of temperature and initial porosity on time to reach s_{90} at 200 kPa

4.4 Differential Settlement

When investigating the final settlement values at locations along a radius it was also noticed that differential settlements can occur under thermal treatment. As shown in Figure 4.18, for a completely surcharge driven consolidation at ambient temperature, the final settlements at different radial locations ultimately reach the same value. However, with coupled mechanical and thermal loading, the ultimate settlement values at different radial locations vary as shown in Figure 4.19. The differences in settlements can be attributed to the differences in steady state temperatures along a radius which can change the magnitude of thermally induced settlement. However, the differential settlement would not be pronounced due to stress redistribution resulting from shear.

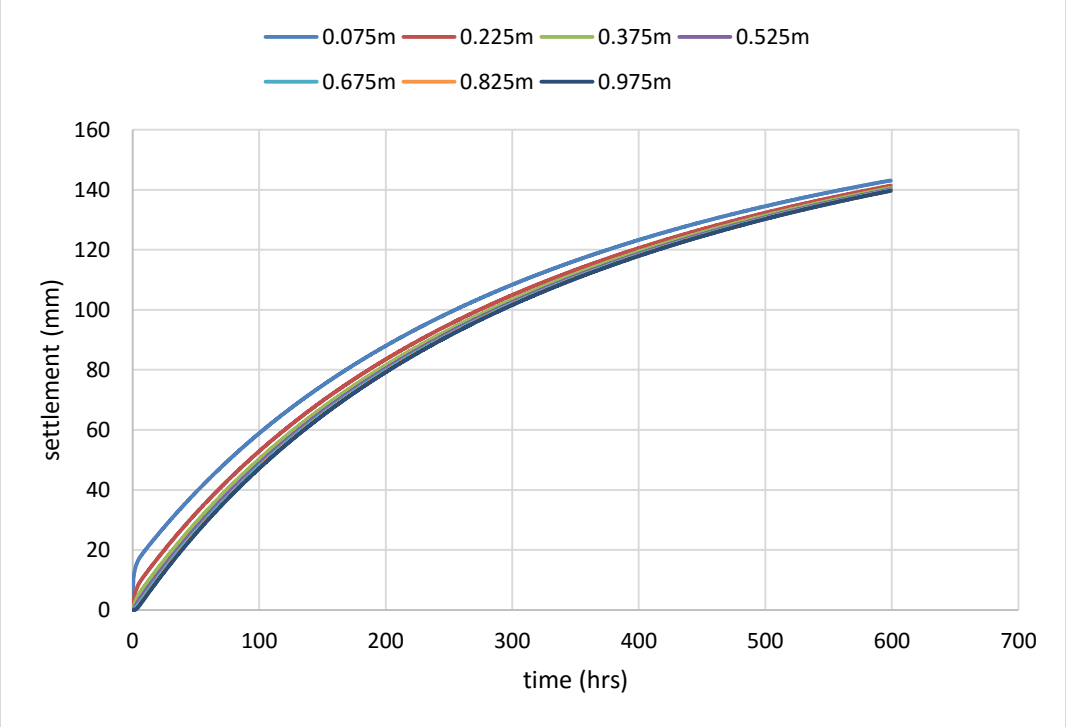

Figure 4.18 Settlement at different radial locations at 100 kPa and 20°C

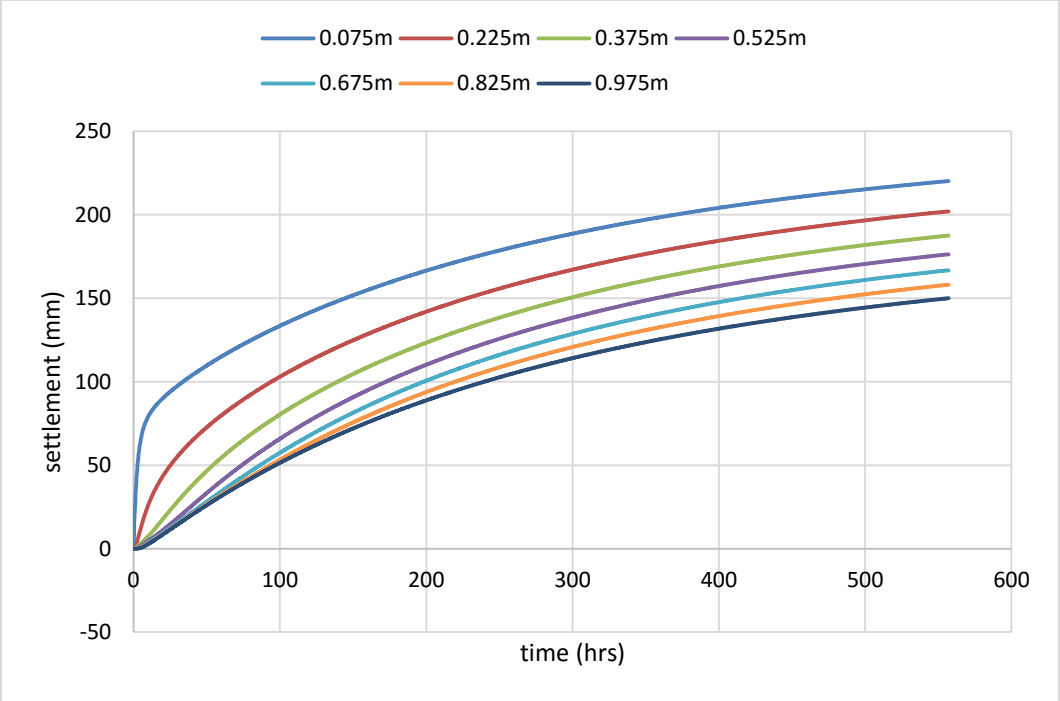

Figure 4.19 Settlement at different radial locations at 100kPa and 90°C

4.5 Expansion in NC Clay

At low initial porosity and relatively low surcharge values, some initial expansion was observed even in NC clays for high temperature increments as shown in Figure 4.20. In the constitutive model developed by Abuel-Naga, Bergado, Bouazza, & Ramana (2007), it is stated that only irreversible contraction is observed in the NC range. However, the above theory was developed considering the isothermal consolidation behavior at elevated temperatures and increasing temperatures at a constant total stress. The simultaneous application of both mechanical and thermal loading was not comprehensively investigated. Although laboratory and field experiments too have been conducted to validate the model, a comprehensive study with varying surcharge loads or initial porosities was not found in the literature. Since the numerical model couples fluid flow with compressibility characteristics of the soil considering

multiple soil elements and simultaneously applies both the mechanical and thermal loading, it was possible to observe this phenomena.

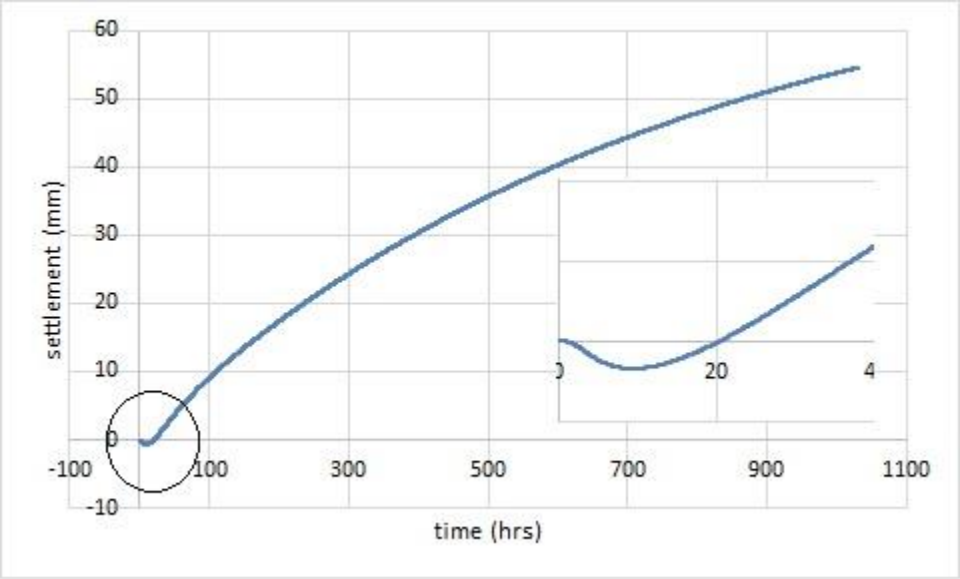

Figure 4.20 Initial expansion observed in NC clay at 0.5m from drain (50 kPa and 70°C)

The reason for this initial expansion can be explained as follows. As discussed in Chapter 1, an increase in temperature can generate thermally induced excess pore water pressure. With the heat source at the drain, locations closer to the drain will get heated sooner than those far away. At initial stages, before the surcharge load is transferred, even the locations further away from the drain will be at pressures closer to hydrostatic pressures. Therefore the flow could also be in the direction away from the drain which could result in an expansion at locations further away from the drain. As the surcharge load continues to transfer, the flow will gradually be directed toward the drain and contraction will begin. The change in flow direction can be observed in Figure 4.21.

This effect can be significant at very low initial porosities and relatively low surcharge loads when subjected to very high temperature increments. For example, for the case run at 90°C under a 50 kPa load, complete expansion was observed at locations further away from the drain. However, by increasing the temperature only up to 70°C, the surcharge up to 100 kPa or the initial porosity up to 0.65 while maintaining the other conditions the same, contraction could be observed. Therefore, it is important to use an appropriate combination of temperature and surcharge for a clay with given initial porosity to obtain a desired output for the settlement.

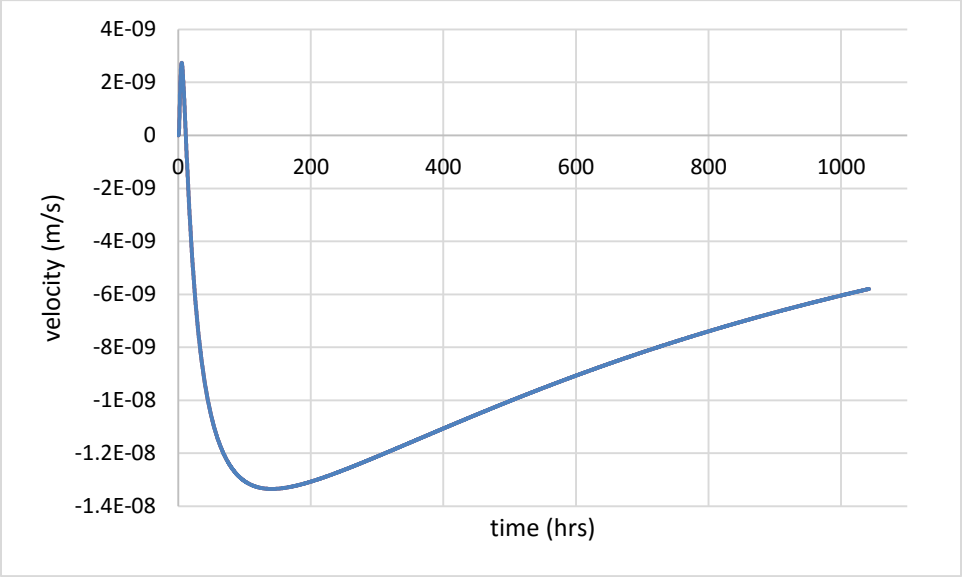

Figure 4.21 Velocity variation for NC clay at 0.5m from drain (50 kPa and 70°C)

4.6 Effects of Cooling

The effect of cooling on settlement was also included in the numerical model. It was assumed that cooling will occur only after the settlement due to heating and surcharge is

complete and the heat source is removed. As stated in literature (Robinet, Rahbaoui, Plas, & Lebon, 1996), the effect on settlement due to cooling is only significant in expansive clays. In non-expansive clays, the settlement resulting from cooling is negligible. For an expansive clay, the magnitude of settlement due to cooling can be as large as the magnitude of settlement generated during the heating process. However, in the results from the model, significant contraction was observed under cooling even with non-expansive soil properties. As the surcharge load increases the contribution to settlement from cooling can be seen to diminish as shown in Figure 4.22.

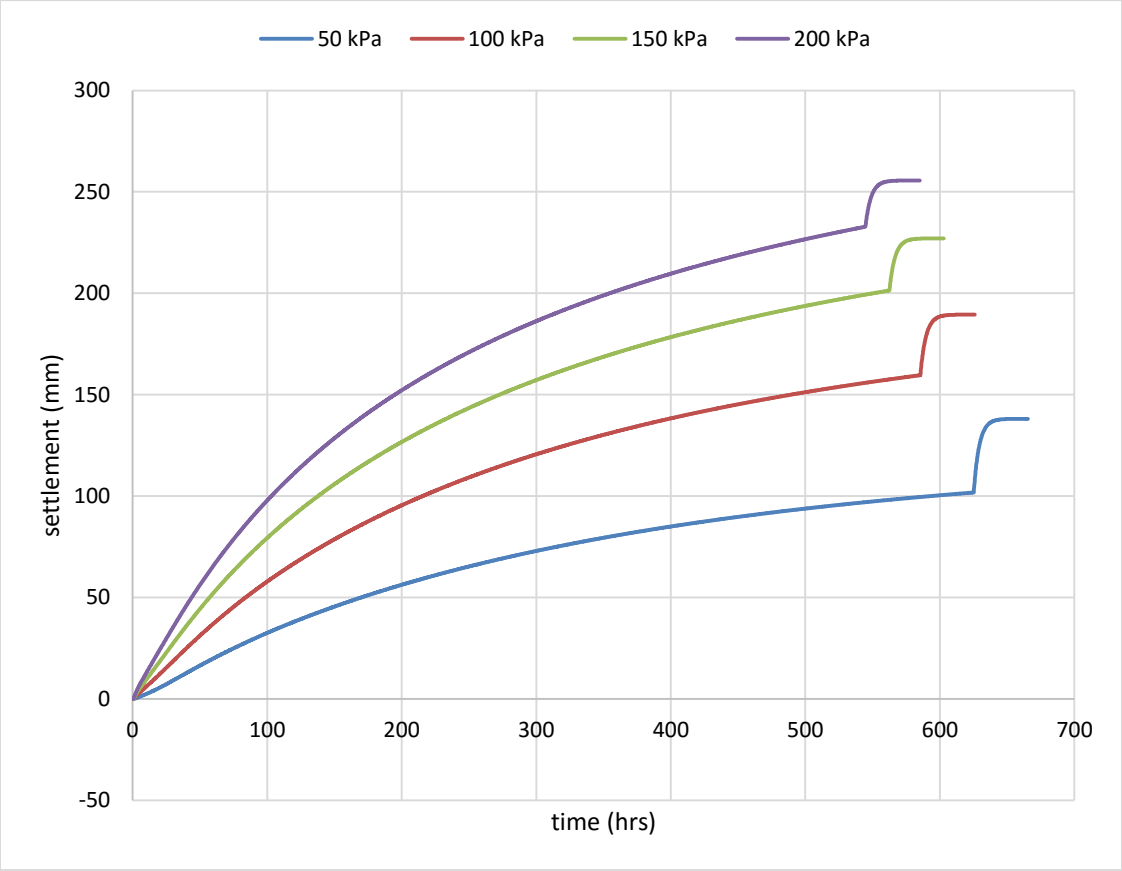

Figure 4.22 Settlement due to cooling at different surcharge loads for 50°C

4.7 Thermally Induced Over Consolidation

It was also discussed in Chapter 1 that an over consolidation state will be induced in NC clays after a heating-cooling cycle, as a result of thermal yielding of the soil. The increased pre consolidation pressure for the corresponding thermal loading can be obtained using equation 25. The percentage increase in the pre consolidation pressure for a soil with an initial maximum pre consolidation pressure of 100kPa and initial porosity of 0.65 subject to varying surcharge loads and temperatures are summarized in Table 4.1. It should be noted that the initial porosity was not meant as a classification parameter for clay but merely an observation made while investigating the parameters affecting the compressibility.

Table 4.1 Percentage increase in pre consolidation pressure

	50 kPa	**100 kPa**	**150 kPa**	**200 kPa**
20°C	40.17%	73.88%	103.6%	129.72%
50°C	51.64%	88.87%	121.31%	149.37%
70°C	58.27%	97.68%	131.89%	161.22%
90°C	64.35%	105.86%	141.82%	172.48%

CHAPTER 5: CONCLUSION

In this research a computational code was developed to investigate the effect of thermal treatment on the consolidation of fine grained soils and to determine ways of optimizing the thermal treatment to expedite consolidation. Based on the results it can be concluded that the magnitude and rate of settlement increase at elevated temperatures for a given surcharge and initial porosity. This increase is more significant at relatively lower surcharges and lower initial porosities.

Some initial expansion can be observed even in NC clays with low initial porosities when subject to very high temperature increments coupled with a relatively low surcharge load. Therefore, an optimum combination of temperature and surcharge should be chosen for a soil with given initial conditions in order to obtain the maximum improvement in the settlement.

Differential settlements can occur during a coupled mechanical and thermal load induced consolidation process due to the differences in the steady state temperatures in the radial direction. The increase in the maximum past pressure after a heating-cooling cycle is mainly dependent on the temperature increment.

The developed numerical model facilitated the investigation of different scenarios. Hence, it was possible to recognize certain new aspects of the thermal treatment process which were not previously investigated in detail. Further experimentation and numerical investigations can be carried out to confirm the predicted behavior. As this technique is still in

its experimental stages, the developed numerical model will provide the framework to determine the viability of its practical applications.

REFERENCES

Abuel-Naga, H. M., Bergado, D. T., & Chaiprakaikeow, S. (2006). Innovative Thermal Technique for Enhancing the Performance of Prefabricated Vertical Drain during the Preloading Process. *Geotextiles and Geomembranes*, 359-370.

Abuel-Naga, H. M., Bergado, D. T., Bouazza, A., & Ramana, G. V. (2007). Volume Change Behaviour of Saturated Clays Under Drained Heating Conditions: Experimental Results and Constitutive Modeling. *Canadian Geotechnical Journal*, 942-956.

Artidteang, S., Bergado, D. T., Saowapakpiboon, J., Teerachaikulpanich, N., & Kumar, A. (2011). Enhancement of Efficiency of Prefabricated Vertical Drains Using Surcharge, Vacuum and Heat Preloading. *Geosynthetics International*, 35-47.

Barron, R. A. (1948). Consolidation of Fine-Grained Soils by Drain Wells. *American Society of Civil Engineers*.

Bergman, T. L., Lavine, A. S., Incropera, F. P., & Dewitt, D. P. (2007). *Fundamentals of Heat and Mass Transfer.* John Wiley & Sons, Inc.

Bird, R. B., Stewart, W. E., & Lightfoot, E. N. (1960). *Transport Phenomena .* John Wiley & Sons, Inc.

Carrier, W. D. (2003). Goodbye, Hazen; Hello, Kozeny-Carman. *ASCE Journal of Geotechnical and Geoenvironmental Engineering*.

Cengel, Y. A., & Cimbala, J. M. (2006). *Fluid Mechanics Fundamentals and Applications.* McGraw-Hill.

Cui, Y. J., Sultan, N., & Delage, P. (2000). A Thermomechanical Model for Saturated Clays. *Canadian Geotechnical Journal*, 607-620.

Hillel, D. (1980). *Fundamentals of Soil Physics.* Academic Press.

Jeyisanker, K., & Gunaratne, M. (2008). *Analysis of Water Seepage Through Earthen Structures using Particulate Approach.* (Doctoral Dissertation). Retrieved from http://scholarcommons.usf.edu/etd/317

Laloui, L., & Cekerevac, C. (2003). Thermo-plasticity of Clays: An Isotropic Yield Mechanism. *Computers and Geotechnics*, 649-660.

Muliphysics Cyclopedia. (n.d.). Retrieved from Comsol: https://www.comsol.com/multiphysics/boussinesq-approximation

Pothiraksanon, C., Bergado, D. T., & Abuel-Naga, H. M. (2010). Full-Scale Embankment Consolidation Test using Prefabricated Vertical Thermal Drains. *Soils and Foundations*, 599-608.

Robinet, J.-C., Rahbaoui, A., Plas, F., & Lebon, P. (1996). A Constitutive Thermomechanical Model for Saturated Clays. *Engineering Geology*, 145-169.

Saowapakpiboon, J., Bergado, D. T., Thann, Y. M., & Voottipruex, P. (2009). Assessing the Performance of Prefabricated Vertical Drain with Vacuum and Heat Preloading. *Geosynthetics International*, 384-392.